The mechanism of supplementary cementitious materials enhancing the water resistance of magnesium oxychloride cement (MOC): a comparison between pulverized fuel ash and incinerated sewage sludge ash

Pingping He[1], Chi Sun Poon[1]*, Ian G. Richardson[2]，and Daniel C.W. Tsang[1]

[1]Department of Civil and Environmental Engineering, The Hong Kong Polytechnic University, Hung Hom, Kowloon, Hong Kong

[2]School of Civil Engineering, University of Leeds, Leeds LS2 9JT, United Kingdom

*Corresponding author: cecspoon@polyu.edu.hk

Abstract: Magnesium oxychloride cement (MOC) pastes incorporating supplementary cementitious materials (SCMs) including pulverized fuel ash (PFA) and incinerated sewage sludge ash (ISSA) were examined by scanning electron microscopy (SEM) and transmission electron microscopy (TEM) with energy dispersive X-ray spectrometry (EDX). The result showed that the mechanism of PFA and ISSA in improving the water resistance of MOC paste is similar, even though the molar ratios of the hydration product in the ISSA-incorporated paste and the PFA-incorporated paste were different. The active phases in PFA or ISSA could react with MgO and produce an amorphous phase (amorphous magnesium aluminosilicate gel), which was interspersed with Phase 5 and changed the morphology of Phase 5 to fibroid or lath-like phases. These fibroid or lath-like phases interlocked with each other and also connected with the amorphous phase in the matrix to form a stable compact structure. Therefore, the water resistance of MOC was improved. The ISSA-blended MOC paste had higher water resistance compared to the PFA-blended MOC, which may be due to the different chemical composition of amorphous phase and the dissolved phosphorus from ISSA.

Keywords: Magnesium oxychloride cement; Water resistance; Microstructure; TEM

1. Introduction

It is known that MOC exhibits many advantageous properties such as high early strength[1, 2], high fire resistance[3], high abrasion resistance[4], etc. It can be used for industrial flooring[5],

ship decks[4], fire protection[3], lightweight panel[2], etc. However, the application of MOC is not widespread due to the poor water resistance. It was reported that the compressive strength of MOC decreased by about 90% when it was immersed in water for 28 days[6]. It was concluded that $Mg(OH)_2$ would be formed as a result of the decomposition of the MOC hydration products-Phase 5($5Mg(OH)_2 \cdot MgCl_2 \cdot 8H_2O$) and Phase 3($3Mg(OH)_2 \cdot MgCl_2 \cdot 8H_2O$)[7] which were the main strength sources of MOC. And the $Mg(OH)_2$ has a much lower strength than that of Phase 5 and Phase 3.Therefore, the compressive strength of MOC decreased when immersed in water. Besides, the length change of MOC mortar was 1.8% after 28 days of water immersion[6], as the hydration of excess MgO resulting the expansion of MOC mortar. The expansion may also lead to crack of specimens and then the reduction of strength.

According to a previous study, the use of SCMs - class F pulverized fuel ash (PFA)[6], glass powder[8], and incinerated sewage sludge ash (ISSA) [9] could improve the water resistance of MOC. The PFA was a pozzolanic waste material generated during the combustion of coal sourced from a local power plant in Hong Kong. GP was obtained by milling recycled glass cullet collected from a local glass recycler (Laputa Eco-Construction Material Co. Ltd.). ISSA was obtained from the sewage sludge incineration center-T park, Hong Kong. The quantitative X-ray diffraction (Q-XRD) result showed that the amorphous content in the MOC paste increased after adding PFA and ISSA (higher than 50% after water immersion for 14 days) and was much higher than the amorphous content in the raw materials (around 10% of the whole mixture). These amorphous phases may be the reaction products between the MOC and Si or Al in SCMs as shown in Table 1. While the Phase 5 in the pure MOC paste decomposed completely during water immersion, the sample prepared with the incorporation of PFA or ISSA still contained certain amount of Phase 5 which was intermixed with some new amorphous phases. This indicated that the new amorphous phases helped to improve the stability of MOC in water. Therefore, it is important to understand the microstructure the amorphous phase in SCMs-blended MOC.

Table 1. Chemical compositions of MgO, PFA and ISSA

Composition	MgO	PFA	ISSA

(% by mass)			
MgO	94.86	4.10	3.21
SiO_2	2.75	45.70	28.34
AlO_3	--	19.55	12.44
Fe_2O_3	0.45	11.72	18.60
CaO	1.60	12.27	10.63
Na_2O	--	1.36	7.43
K_2O	--	1.71	1.92
SO_4	0.24	1.82	6.22
P_2O_5	--	--	9.92

SEM/EDX has been used previously to characterize the morphology of MOC incorporating PFA and ISSA[6, 9]. By using SEM-EDX, it was found that the morphologies of the hydration products were changed after adding ISSA and PFA. The main product in a pure MOC was the needle-like Phase 5, while the hydration products were present as flat and wide plates containing Si and Al in the PFA/ISSA- blended cement. However, due to nature of SEM and the limitation of the sample preparation, it is difficult to characterize the elemental compositions and the morphology of the new amorphous phase using SEM-EDX. TEM is an effective technique to investigate the microstructure of intermixed phases[10, 11] and to distinguish the amorphous phases from the crystalline phases. Therefore, the objective of this study is to investigate the morphology and distribution of the amorphous phases formed in MOC incorporating PFA and ISSA by using TEM. EDX was employed to further investigate the elemental compositions of the products formed in the PFA/ISSA-blended MOC pastes.

2. Experimental program

The materials used were as follows: Light-burned magnesia powder (MgO), Bischofite ($MgCl_2$• $6H_2O$), Class F PFA, and ISSA. The details of these materials have been given in our previous study[6, 9]. The bischofite was mixed with water to ensure complete dissolution and then poured into the mixing bowl before MgO was added. The molar ratio of MgO/ $MgCl_2$ and H_2O/ $MgCl_2$ were 9 and 10 respectively. The PFA and ISSA was respectively used to replace MgO at a dosage level of 30% by mass of MgO. The $MgCl_2$• $6H_2O$ was firstly dissolved in water forming a clear solution and then mixed with the dry powders thoroughly for 3 min to obtain a uniform paste. The solubility of $MgCl_2$• $6H_2O$ is 54.3g/100ml at 20°C. Therefore, 1 mol $MgCl_2$ can be completely dissolved in 10 mol water. The MOC paste were cast into 20mm*20mm*20mm steel molds and placed in an air curing chamber at 25°C (RH=50%) for 14 days after demolding followed by water immersion at 20±1°C. The average compressive strength of six cube samples was determined before and after water immersion using a Denison compression machine at a loading rate of 1 kN/s. The fractured surface of the specimens was coated with gold and observed with a JEOL Model JSM-6490 SEM. The samples for TEM tests were first cast in plastic cylindrical tubes, and sections of 2 mm long were cut from the cylinder, polished down to 30 μm, thick and glued between 3 mm diameter nickel grids. Then they were argon ion-beam milled and carbon coated. The bright field images and chemical analyses were collected using a field emission transmission electron microscope (FEI Tecnai TF20 FEGTEM/STEM operating at 200 kV and fitted with an Oxford Instruments INCA 350 EDX system and 80 mm X-Max SDD detector). The detailed methodologies for the TEM examinations have been reported in previous studies [12, 13]. The EDX results were calculated based on the average values of 10 points with the ratios of standard deviations/average values of less than 0.5.

3. Results and discussion

3.1. Compressive strength

The compressive strengths of the MOC pastes are shown in Fig. 1(A14 means 14 days of air curing, W28 means 14 days of air curing followed by 28 days of water immersion). It can be seen that MOC pastes showed high compressive strength before water immersion.

The compressive strength of control MOC paste was about 160 MPa after 14 days of air curing. The incorporation of PFA and ISSA slightly decreased the strength, but the strength of PFA-blended MOC was still higher than 100 MPa. It can be observed that the compressive strengths of all the paste mixes decreased after water immersion for 28 days due to the decomposition of main hydration products-Phase 5 and Phase 3 which were the main strength sources of MOC mixtures. However, the MOC pastes incorporating PFA or ISSA had lower strength loss compared to the control pastes. The compressive strength was decreased by about 90% after 28 days of water immersion for the control samples, while it was 27% and 13% for the MOC pastes incorporating PFA and ISSA respectively. This indicated that PFA and ISSA could significantly increase the water resistance of MOC.

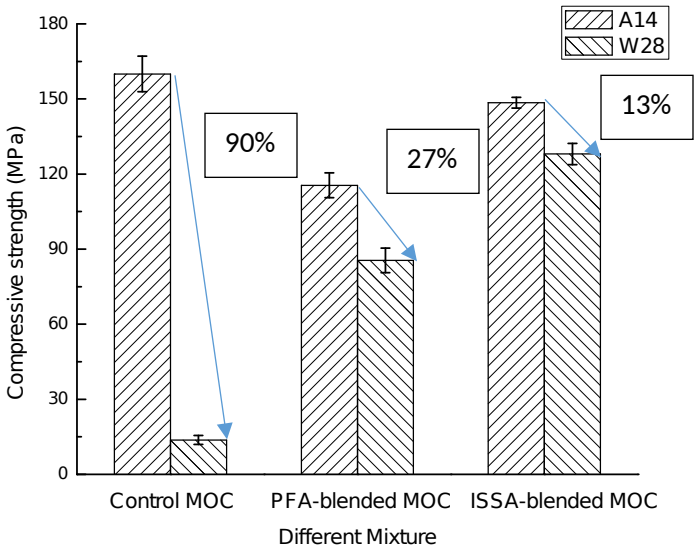

Fig. 1 Compressive strength of MOC paste before and after water immersion

3.2. SEM and TEM

3.2.1. Control MOC

The morphology of the MOC paste after 14 days of air curing is displayed in Fig.2. The SEM micrograph (Fig.2a) shows that the surface of the cement paste was

covered with a large quantity of needle-like crystals, which were typical of Phase 5 and this was confirmed by EDX analysis result (molar ratio of Mg to Cl was 3). TEM was used to further examine the particle size, crystallinity and morphology of the samples with a higher magnification as shown in Fig.2b, which was a bright field image of the MOC paste. It can be estimated that the width of this needle-like phase was about 30-70 nm. A gauzelike homogeneous morphology can be observed (Fig.3 a) after further increasing the magnification (Fig. 2b). The corresponding selected area electron diffraction (SAED) pattern of the needle-like phase is shown in Fig. 3b. A small tip ("beam stopper") above the observation screen was inserted to cover the bright spot in the center to avoid damaging the camera[14]. It shows the (0 1 2), (4 0 -1), (0 1 3), and (5 1 0) lattice spacing value of 2.42 Å, 2.39 Å, 1.97 Å, and 1.54 Å respectively. This diffraction pattern indicated the needle-like phase in Fig.2b is Phase 5.

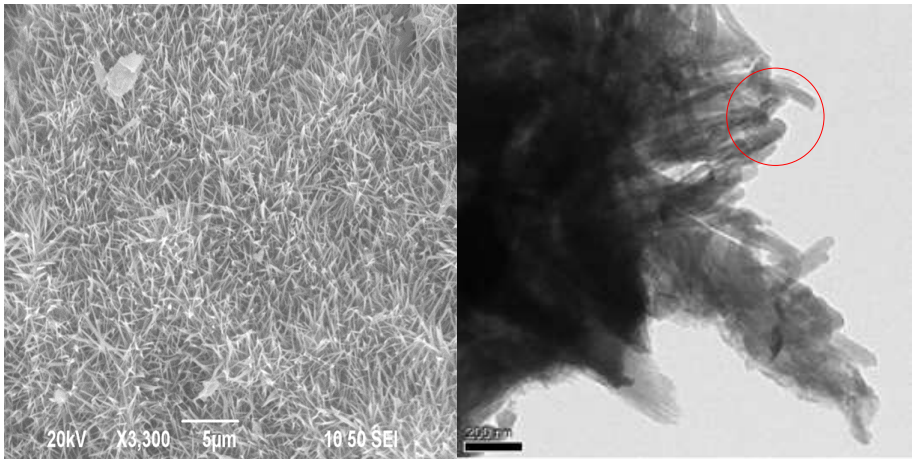

(a) **(b)**

Fig. 2 SEM image (a) and TEM image (b) of MOC

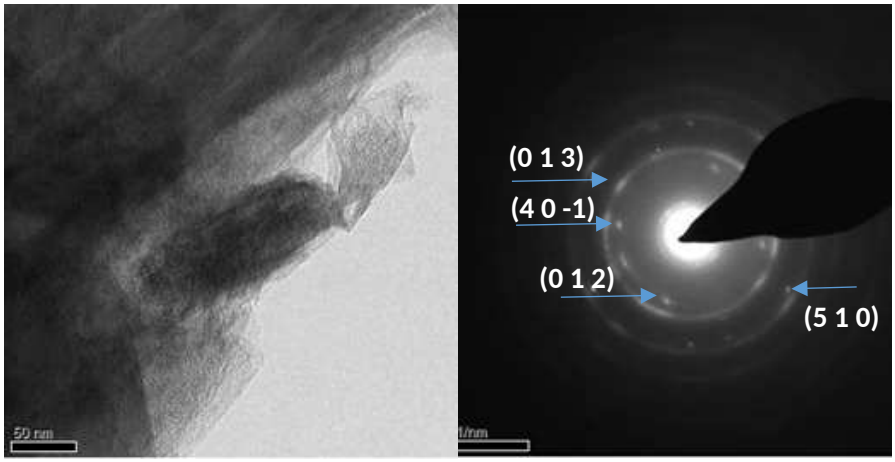

(a) **(b)**

Fig. 3 TEM image (a) and selected area electron diffraction pattern (b) from the selected region in Fig.2

3.2.2. MOC incorporating PFA

The incorporation of PFA in the MOC mix was found to influence the hydration behavior and led to differences in the microstructure of the hydration products. It seems that based on SEM the main hydration product was changed to a lath-like phase as shown in Fig.4a. In order to avoid intermixing, TEM was used as shown in Fig. 4b to reveal the detailed microstructure. The width of this lath-like phase was approximately 150-250 nm. With further increasing in magnification (Fig.5a), dark-grain structures could be observed. Electron diffraction analysis of this lath-like phase showed spotty ring patterns (Fig.5b), which can be interpreted as semi-crystalline particles. The EDX detected Si and Al in addition to Mg and Cl, among which the Mg/Al/Si/Cl atomic ratio was 13.8:2.3:0.77:1. This indicates an amorphous magnesium aluminosilicate phase was formed which interspersed with the crystalline particles-Phase 5.

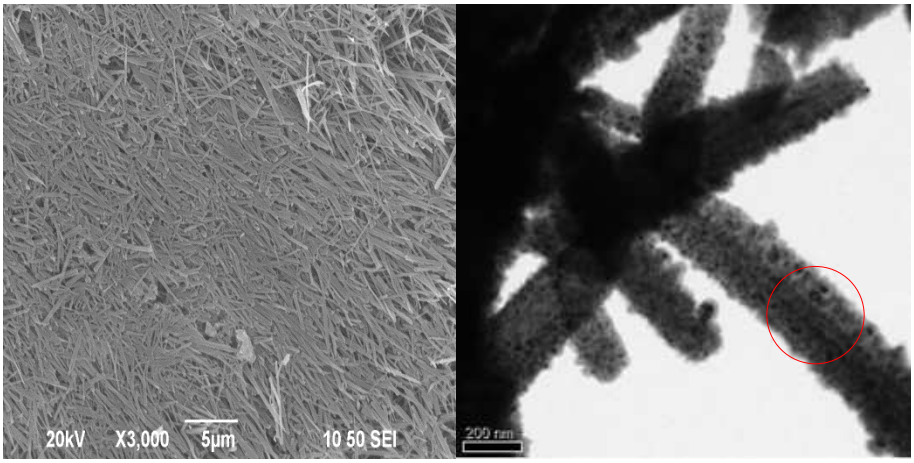

(a) **(b)**

Fig. 4 SEM image (a) and TEM image (b) of MOC incorporating PFA

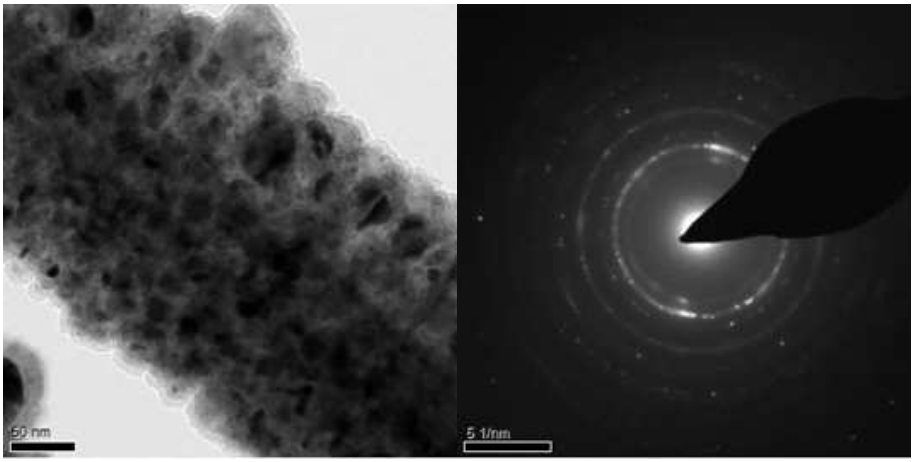

(a) **(b)**

Fig. 5 TEM image (a) and selected area electron diffraction pattern (b) from the selected region in Fig.4

Apart from the lath-like phase, a foil-like phase could also be observed in the TEM image of the MOC paste incorporating PFA as shown in Fig. 6. Electron diffraction analysis of this foil-like phase showed a faint, diffused ring, which is associated with amorphous particles. The EDX detected Mg, Al, Si in a molar ratio of 14.2:2.8:1. As reported in a previous Q-XRD study[6], the PFA could improve the

water resistance of MOC paste due to the formation of an amorphous phase. But the microstructure of this amorphous phase was not clear in the SEM image as it was present as an intermixed structure. The TEM technique can analyze the individual particles, which avoids interferences from other phases. From Figs. 4-6, it can be seen that the silicate and aluminate in PFA could react with the MOC and the product was formed not only in the matrix individually but also interspersed with the crystalline particle-Phase 5. These changed the morphology of Phase 5.

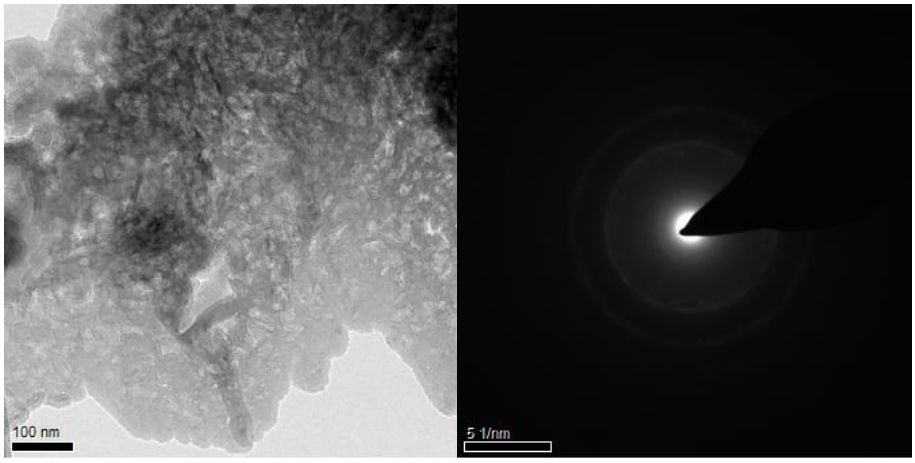

(a) **(b)**

Fig. 6 TEM image (a) and selected area electron diffraction pattern (b) of MOC incorporating PFA

3.2.3. MOC incorporating ISSA

When incorporating ISSA in the MOC, the main hydration product in the MOC paste was with a short needle like morphology, forming a compact matrix as shown in the SEM image (Fig.7a). The width of this fibroid phase was around 70-120 nm according to the TEM image in Fig. 7b. With increased magnification, a dark-grain structure similar to that in Fig. 5a can be observed (Fig.8). But it was much thinner than that in the PFA-incorporated MOC paste. The EDX detected a molar ratio of Mg, Si, and Cl of 10.6:0.7:1, which indicated that the silicate in ISSA could react with MgO and the product was dispersed on the needle-like Phase 5. In addition to

the fibroid phase, granular particles could be observed as well, which was an amorphous phase as shown in Fig.9. The EDX detected a molar ratio of Mg, Si, and Cl of 20:2.1:1.

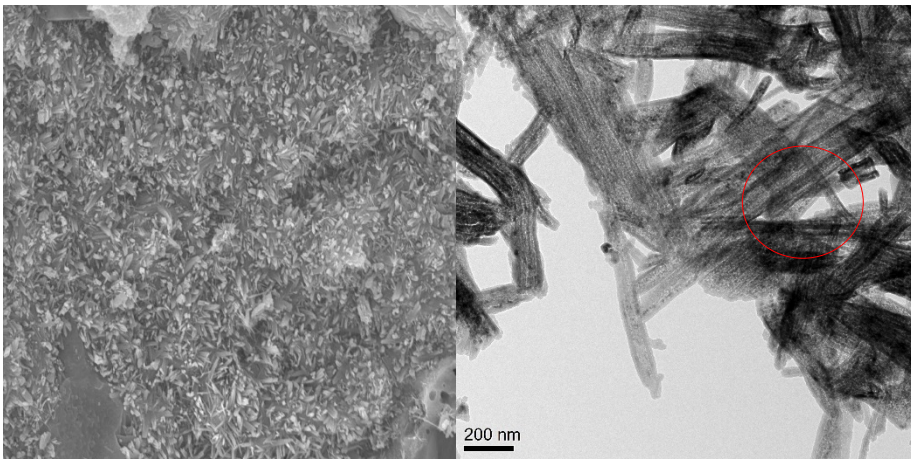

(a) **(b)**

Fig. 7 SEM image (a) and TEM image (b) of MOC incorporating ISSA

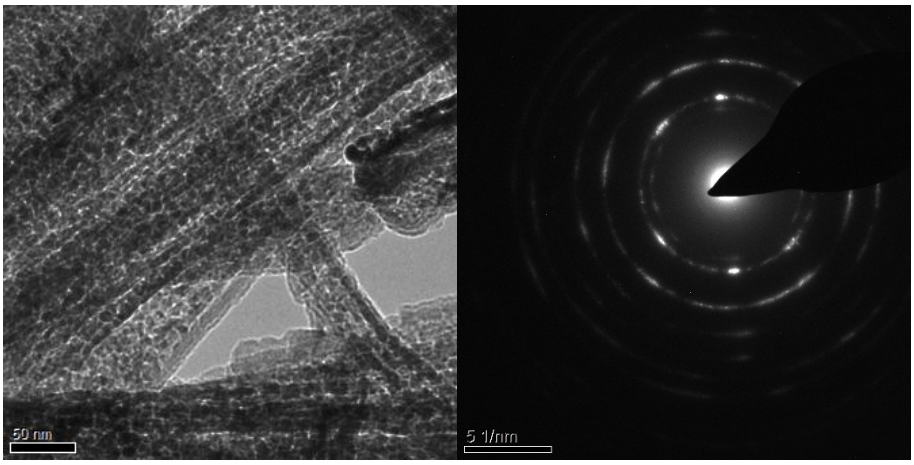

(a) **(b)**

Fig. 8 TEM image (a) and selected area electron diffraction pattern (b) from the selected region in Fig.7

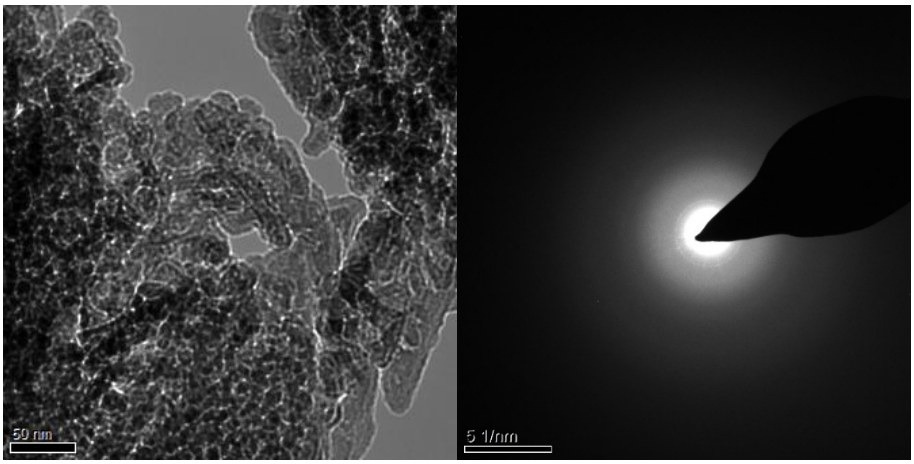

Fig. 9 TEM image (a) and selected area electron diffraction pattern (b) of MOC incorporating ISSA

4. Discussion

Table 2. Summary of results of hydration products formed and water resistance of different MOC mixtures

	Control MOC	PFA-blended MOC	ISSA-blended MOC
Compressive strength (14 days of air curing)	165±7.5MPa	112±4.3MPa	150±2.2MPa
Strength retention coefficient (water immersion for 28 days)	10%	73%	87%

Expansion [6, 9] (water immersion for 28 days)	1.80±0.08%	0.60±0.02%	0.25±0.01%
SEM micrographs of hydration products	needle-like phase	flat and wide plates	lath-like structure
TEM micrographs of hydration products	thin needle	a) lath-like phase and b) foil-like phase	a) fibroid-like structure and b) granular-like structure
EDX (TEM) results of hydration products (atomic ratio)	Mg:Cl=3	a) Mg:Al:Si:Cl=13.8:2.3:0.77:1 b) Mg:Al:Si=14.2:2.8: 1	a) Mg:Si:Cl=10.6:0.7:1 b) Mg:Si:Cl=20:2.1:1

Note: Strength retention coefficient was calculated as the ratio between the compressive strength of the specimens before water immersion to the residual compressive strength of the specimens after water immersion for the given period of time. When calculating the expansion, the length of the specimens before water immersion was recorded as the initial length.

As can be seen from Table 2, the MOC paste had high compressive strength and the strength was 165MPa after 14 days of air curing. However, the compressive strength decreased significantly when immersed in water due to the decomposition of hydration products (Phase 3 and Phase 5) and the strength retention coefficient was only 10% after 28 days of water immersion. When adding PFA or ISSA, the compressive strength decreased slightly during air curing (112MPa and 150 MPa respectively). However, the strength retention coefficient after immersion in water significantly increased and reached more than 70%. Based on our past test results[6] , the expansion of pure MOC mortar was 1.8% after 28 days of water immersion which was due to the hydration of excess MgO. This value was 0.6% and 0.25% for the MOC mortars incorporating PFA and ISSA respectively, which was due to the reduction of excess MgO and the increased stability of the hydration products adding PFA or ISSA. The compressive strength results and length change results showed that PFA and ISSA could

significantly improve the water resistance of MOC mixture and ISSA induced better improvement of the water resistance.

According to our previous study[6, 9] ,the hydration product of pure MOC paste was Phase 5 and no new crystalline phase was found after adding PFA and ISSA. However, the content of amorphous phases in the PFA/ISSA incorporated MOC pastes was much higher after air curing for 14 days than that in the raw materials. Therefore, the amorphous phases generated after adding PFA and ISSA maybe the reason for the improvement of water resistance of MOC.

The ISSA-blended MOC paste had higher water resistance compared to the PFA-blended MOC paste, which might be due to three reasons. Firstly, ISSA-blended mixture had a higher content of amorphous phases. According to our previous study, the Phase 3 and Phase 5 in pure MOC paste decomposed completely after 28 days of water immersion. However, a certain amount of Phase 3, Phase 5 and amorphous phases were detected after water immersion in the MOC paste incorporating PFA or ISSA, indicating that the amorphous phases were stable in water, interlocked with Phase 3 and Phase 5 and protected them from decomposition. The initial amorphous phase contents in the raw materials preparing the MOC pastes with ISSA or PFA incorporation were similar (around 10% of the total raw materials), but the ISSA-blended MOC paste had much higher amorphous content (76%) compared to PFA-blended MOC (24.7%) after 14 days of air curing. Therefore, the higher amorphous phase content produced might be one of the reasons that the ISSA-blended MOC had better water resistance.

The second reason may be due to the different chemical compositions of the hydration products. It can be seen from Table 2 that both of the hydration products in the PFA-blended MOC and the ISSA-blended MOC were wider and bigger than that in pure MOC paste according to SEM micrographs. TEM micrographs showed that the amorphous phases interspersed with Phase 5 and changed the morphology of Phase 5 from a needle-like structure to a lath-like structure. Besides, the amorphous phase could be observed separately in the matrix. The amorphous phase in the PFA-blended MOC contained Mg, Al and Si in an atomic ratio of 14.2:2.8:1. While the amorphous phase in the ISSA-blended MOC contained Mg, Si and Cl in an atomic ratio of 20:2.1:1. The different chemical compositions of the amorphous phase may result in the different morphologies of the hydration products and water resistance.

The third reason may be the phosphorus (P) content in ISSA-blended MOC mixture. The pH of the pore solution in MOC paste was about 10-11[15], and the dissolution of P was 5-10 mmol/L when using $Na(OH)_2$ to extract ISSA under this pH range[16]. It was reported that a small amount of phosphate (0.74-1% of MOC paste) could significantly improve the water resistance of MOC[7]. Therefore, the P extracted from ISSA might also had positive effects on improving the water resistance of MOC. However, P was not detected in the ISSA-blended MOC paste, which might be due to the small concentration of P (around 3% in the raw materials).

The MOC deteriorates significantly under moist climate due to the decomposition of hydration products- Phase 3 and Phase 5, which might lead to the leaching of free chloride and the corrosion of steel when it is used in reinforced concrete. When adding PFA and ISSA, the amorphous alumino-silicate gel was produced by the reaction between the reactive SiO_2 and Al_2O_3 contents in PFA/ISSA and MOC. This gel product is associated with large surfaces which interlocked with Phase 3 and Phase 5, changed the morphology of the hydration products, and formed a network to protect them from decomposition. That is why a certain amount of Phase 5 could still be observed after water immersion for 28 days in the MOC incorporating PFA and ISSA and the strength retention coefficient was much higher than the pure MOC. Even though the chloride bonding type in the amorphous gel was not clear, it can be suggested that the leaching of free chloride was significantly prohibited. Therefore, the chance of steel corrosion might be decreased. The potential leaching of free chloride and its impact on metal corrosion still need to be further studied.

5. Conclusion

MOC showed poor water resistance due to the instability of the hydration products in water. Using PFA or ISSA could significantly improve the water resistance. New amorphous phases were observed in PFA or ISSA blended MOC, which may be the reason why they improved the water resistance.

The morphologies of magnesium oxychloride cement incorporating PFA and ISSA were examined using SEM and TEM/EDX. The SEM result showed that the main hydration product in MOC paste was needle-like crystalline- Phase 5. When adding PFA and ISSA, the main

hydration product present was with a lath -like structure. This change in structure was the reason for the improvement of water resistance of MOC. But it was difficult to clearly observe the microstructure and elemental compositions of this structure by SEM due to the intermixing of the different phases. The TEM results showed that two phases were formed when adding PFA and ISSA, including a lath-like/fibroid-like phase and an amorphous phase. The former phase was much bigger than the needle-like Phase 5 and contained Mg, Si (Al) and Cl, indicating that the product produced due the reaction between PFA/ISSA and MgO interspersed with Phase 5 and changed the morphology of Phase 5. The latter amorphous phase was a magnesium aluminosilicate. These two phases interlocked with each other and formed a stable structure which was resistance to the dissolution of water. The amorphous phase in the ISSA-blended MOC contained Mg, Si and Cl, while the PFA-blended MOC contained Mg, Al, Si. The difference in chemical compositions of amorphous phases may be the reason that the former mixture had better water resistance than the latter one. Besides, the dissolved P from ISSA may also help to improve the water resistance of the ISSA-blended MOC. However, P was not detected from EDX result, which might be related to the low concentration of P in the sample. The effect of P on the water resistance of MOC needs to be further investigated. Moreover, the bonding type and leaching behavior of chloride in the hydration products also needs further studies.

Acknowledgement

The authors would like to acknowledge the financial support from the Construction Industry Council.

References

1. Y. Li, H. Yu, L. Zheng, J. Wen, C. Wu, and Y. Tan, Compressive strength of fly ash magnesium oxychloride cement containing granite wastes. Construction and Building Materials, 2013. **38**: p. 1-7.
2. P. He, M.U. Hossain, C.S. Poon, and D.C. Tsang, Mechanical, durability and environmental aspects of magnesium oxychloride cement boards incorporating waste wood. Journal of Cleaner Production, 2018. **207**: p. 391-399.
3. J. Montle and K. Mayhan, The role of magnesium oxychloride as a fire-resistive material. Fire Technology, 1974. **10**(3): p. 201-210.
4. A. Misra and R. Mathur, Magnesium oxychloride cement concrete. Bulletin of Materials Science, 2007. **30**(3): p. 239-246.

5. G. Li, Y. Yu, J. Li, Y. Wang, and H. Liu, Experimental study on urban refuse/magnesium oxychloride cement compound floor tile. Cement and Concrete Research, 2003. **33**(10): p. 1663-1668.
6. P. He, C.S. Poon, and D.C. Tsang, Effect of pulverized fuel ash and CO2 curing on the water resistance of magnesium oxychloride cement (MOC). Cement and Concrete Research, 2017. **97**: p. 115-122.
7. D. Deng, The mechanism for soluble phosphates to improve the water resistance of magnesium oxychloride cement. Cement and Concrete Research, 2003. **33**(9): p. 1311-1317.
8. P. He, C.S. Poon, and D.C. Tsang, Comparison of glass powder and pulverized fuel ash for improving the water resistance of magnesium oxychloride cement. Cement and Concrete Composites, 2018. **86**: p. 98-109.
9. P. He, C.S. Poon, and D.C. Tsang, Using incinerated sewage sludge ash to improve the water resistance of magnesium oxychloride cement (MOC). Construction and Building Materials, 2017. **147**: p. 519-524.
10. I. Richardson, J. Skibsted, L. Black, and R.J. Kirkpatrick, Characterisation of cement hydrate phases by TEM, NMR and Raman spectroscopy. Advances in Cement Research, 2010. **22**(4): p. 233-248.
11. I. Richardson, The nature of the hydration products in hardened cement pastes. Cement and Concrete Composites, 2000. **22**(2): p. 97-113.
12. I. Richardson and G. Groves, Microstructure and microanalysis of hardened ordinary Portland cement pastes. Journal of Materials Science, 1993. **28**(1): p. 265-277.
13. E. Tajuelo Rodriguez, I. Richardson, L. Black, E. Boehm-Courjault, A. Nonat, and J. Skibsted, Composition, silicate anion structure and morphology of calcium silicate hydrates (CSH) synthesised by silica-lime reaction and by controlled hydration of tricalcium silicate (C3S). Advances in Applied Ceramics, 2015. **114**(7): p. 362-371.
14. J. Thomas and T. Gemming, *Analytical transmission electron microscopy: an introduction for operators*. 2014: Springer Science & Business.
15. Z. Li and C. Chau, Influence of molar ratios on properties of magnesium oxychloride cement. Cement and Concrete Research, 2007. **37**(6): p. 866-870.
16. L. Fang, J.-s. Li, S. Donatello, C. Cheeseman, Q. Wang, C.S. Poon, and D.C. Tsang, Recovery of phosphorus from incinerated sewage sludge ash by combined two-step extraction and selective precipitation. Chemical Engineering Journal, 2018. **348**: p. 74-83.